Received: 1 May 2020 | Accepted: 11 June 2020

DOI: 10.1111/ppa.13238

Plant Pathology WILEY

ORIGINAL ARTICLE

Estimating the epidemiology of emerging *Xylella fastidiosa* outbreaks in olives

Steven M. White[1] | Juan A. Navas-Cortés[2] | James M. Bullock[1] | Donato Boscia[3] | Daniel S. Chapman[4]

[1]UK Centre for Ecology & Hydrology, Wallingford, UK

[2]Consejo Superior de Investigaciones Científicas (CSIC), Instituto de Agricultura Sostenible (IAS), Córdoba, Spain

[3]CNR, Istituto per la Protezione Sostenibile delle Piante (IPSP), Bari, Italy

[4]Biological and Environmental Sciences, University of Stirling, Stirling, UK

Correspondence
Steven M. White, UK Centre for Ecology & Hydrology, Wallingford, OX10 8BB, UK.
Email: smwhit@ceh.ac.uk

Funding information
H2020 Marie Skłodowska-Curie Actions, Grant/Award Number: 734353; Horizon 2020 Framework Programme, Grant/Award Number: 635646 and 727987

Abstract

Xylella fastidiosa is an important insect-vectored bacterial plant pathogen with a wide host range, causing significant economic impact in the agricultural and horticultural industries. Once restricted to the Americas, severe European outbreaks have been discovered recently in Italy, Spain, France, and Portugal. The Italian outbreak, detected in Puglia in 2013, has spread over 100 km, killing millions of olive trees, and is still expanding. To date, quantified assessment of important epidemiological parameters useful for risk assessment and management, such as transmission rates, symptomless periods, and time to death in field populations, has been lacking. This is due to the emergent and novel nature of the outbreak and length of time needed to monitor the course of disease progression. To address this, we developed a Bayesian method to infer epidemiological parameters by fitting and comparing compartmental epidemiological models to short snapshots of disease progression observed in multiple field plots. We estimated that each infected tree with symptoms is able to infect around 19 trees per year (95% credible range 14–26). The symptomless stage was estimated to have low to negligible infectivity and to last an average of approximately 1.2 years (95% credible range 1.0–1.3 years). Tree desiccation was estimated to occur approximately 4.3 years (95% credible range 4.0–4.6 years) after symptom appearance. However, we were unable to estimate the infectiousness of desiccated trees from the data. Our method could be used to make early estimates of epidemiological parameters in other emerging disease outbreaks where symptom expression is slow.

KEYWORDS

epidemiological model, *Olea europea*, olive quick decline syndrome, *Philaenus spumarius*, SIR, *Xylella fastidiosa* subsp. *pauca*

1 | INTRODUCTION

Emerging infectious diseases and invasive species are of significant global concern for economies and public health, and are on the rise due to socioeconomic, ecological, and environmental factors, such as human population density and growth, drug resistance, and host richness (Jones *et al.*, 2008). In plant health, diseases such as European ash dieback (Gross *et al.*, 2014) and sudden oak death

(Grünwald *et al*., 2019) have spread to vast parts of the globe, causing death to millions of plants in the process. However, at the start of an outbreak, decision-making processes are less likely to be underpinned by epidemiological information and there is considerable uncertainty around the impact and relative advantage of different disease control measures (Morgan, 2019). Therefore, there is a clear need to develop rapid epidemiological understanding for decision makers.

Xylella fastidiosa is a bacterial plant pathogen with a wide host range of over 500 species (European Food Safety Authority, 2020). It has had a significant impact on agricultural and horticulture trade around the globe and is economically (Tumber *et al*., 2014) and socially (Almeida, 2016) costly. *X. fastidiosa* is a xylem-limited gram-negative bacterium and the recognized agent of a number of severe and economically important diseases, including Pierce's disease of grapevines, citrus variegated chlorosis (CVC), almond leaf scorch, and other disorders of perennial crops and landscape plants (Purcell and Hopkins, 1996). In California alone, it has been estimated that Pierce's disease directly costs the grape-growing industry $104 million per year in reduced yield, management costs, and regulatory costs (Tumber *et al*., 2014). Once restricted to the Americas, a new invasive strain, *X. fastidiosa* subsp. *pauca* ST 53, the causal agent of olive quick decline syndrome (Saponari *et al*., 2013), was discovered near Gallipoli, southern Italy, in October 2013 (Loconsole *et al*., 2014). Since the initial outbreak, the disease has spread through a large proportion of the olive trees (*Olea europaea*) in southern Puglia (Martelli, 2016). A recent estimate suggests there are 4 million unproductive heavily infected or dead olive trees, representing a 10% loss of Italian olive oil, which equates to an economic loss of approximately €390 million (Italia Olivicola, 2019). If left unchecked, it has been estimated that olive-producing countries could lose billions of euros to the disease (Schneider *et al*., 2020). Other strains and outbreaks of the bacterium have since been discovered in other host plants in Spain, France, other regions of Italy (Tuscany), and Portugal (EFSA Panel on Plant Health, 2019a). These detected outbreaks demonstrate multiple and independent introductions because the strains are distinct (Sicard *et al*., 2018; Saponari *et al*., 2019).

The bacterium is generally transmitted by various widespread species of xylem-feeding insect vectors (Homoptera, Auchenorrhyncha) (Cornara *et al*., 2017). Specifically, in olives in Puglia, Italy, *X. fastidiosa* subsp. *pauca* is mainly vectored by the froghopper *Philaenus spumarius* (Saponari *et al*., 2014b). Currently, there is no known cure for this deadly disease of olives once the tree is infected (EFSA Panel on Plant Health, 2019b), and the only approaches for control are to destroy the host trees and limit spread by creating buffer zones around them, or managing the insect vector population by insecticides or removal of their weed habitats (EFSA Panel on Plant Health, 2019a). The outbreak in Puglia, Italy, is characterized by extensive leaf scorch and dieback, mainly in olive trees, although other cultivated and wild hosts such as oleander (*Nerium oleander*), almond (*Prunus dulcis*), myrtle-leaf milkwort (*Polygala myrtifolia*), and coastal rosemary (*Westringia fruticosa*) can also harbour the bacterium (Saponari *et al*., 2013, 2014a).

A particular challenge posed by *X. fastidiosa* subsp. *pauca* in olives is its apparently long symptomless period before the appearance of leaf browning, dieback, and eventual death of the plant. Under laboratory conditions (e.g., artificial inoculation and constant greenhouse environment) symptoms can start to appear after a period of 14 months (c.1.2 years), although this depends on environment and olive cultivar (Saponari *et al*., 2017; EFSA Panel on Plant Health, 2019a). However, the symptomless period under field conditions has yet to be formally quantified. This is an important parameter to estimate because the visualization of symptoms is key for policy implications in transporting olive trees, and containment and control measures (e.g., Decision [EU] 2015/789 and Decision [EU] 2017/2352); these measures include establishing a demarcated area around detected infected areas with specific requirements associated with plant movement into or within the EU, surveillance, plant removal, and other management measures including agricultural practices to control vector populations. Furthermore, while new remote-sensing technologies are being developed to identify infected plants (Zarco-Tejada *et al*., 2018), current surveillance strategies and grower/public awareness rely heavily on visual detection of the symptoms, sampling, and laboratory testing (EFSA Panel on Plant Health, 2019a). Therefore, ascertaining the symptomless lag under field conditions will help to better inform effective policy.

Host to host transmission is one of the key determinants of the speed at which *X. fastidiosa* spreads locally and in the landscape (White *et al*., 2017), but quantification of this process has so far been lacking in olives. It has been shown that within-host bacterial colonization and build-up to infectious levels can take some time (up to a year; Saponari *et al*., 2017), which is likely to affect vector acquisition over the infection period, with symptomless plants being less infective. However, extrapolation from laboratory studies of between-host transmission to the field is not straightforward because the vectors are polyphagous and show distinct seasonal dynamics and behaviour (Cornara *et al*., 2017). An additional complexity is that as the symptoms progress, during which the bacterium propagates and greater numbers of the olive branches die back, the olive tree may become less attractive to the insect vector and thus the propensity for between-host infection may drop. Furthermore, the rate at which host plants become desiccated has also not been formally established. In general, the effects of these complexities for predicting *X. fastidiosa* outbreaks in olives are unknown (but see Daugherty and Almeida, 2019, for outbreaks in grapevines), and simple models that do not allow for this variation may fail to accurately estimate disease dynamics.

In this paper, we aim to address these gaps in our knowledge by fitting epidemiological mathematical models to observed field data, and performing model selection to balance best model fit against model complexity. In doing so, we aim to quantify the underlying epidemiological parameters in the *X. fastidiosa* subsp. *pauca* Puglian outbreak that are essential for accurate pest risk assessment and effective control strategy planning. We also reveal the sensitivity of the models to each of these parameters and how they contribute to the overall epidemic.

2 | MATERIALS AND METHODS

2.1 | Epidemiological model

Our aim is to model the epidemiological dynamics of *X. fastidiosa* subsp. *pauca* in Puglian olive groves. Previous models of *X. fastidiosa* dynamics (White *et al*., 2017; Abboud *et al*., 2019; Daugherty and Almeida, 2019) have generally assumed simple tree to tree infection growth dynamics (e.g., logistic- or Gompertz-type growth models of the number or proportion of infected host plants), or used a simplified compartmental Susceptible-Infected (SI) model that omits critical features of the *X. fastidiosa* epidemiology, such as the symptomless period and host mortality rate (Soubeyrand *et al*., 2018). Our aim is to build a more realistic model that captures additional details of the infection process using a deterministic discrete-time modified compartmental model, adapted to the particular epidemiology of *X. fastidiosa* subsp. *pauca* infection of olive trees. A discrete time model rather than a continuous time one was used because the annual forcing of transmission by seasonal vector populations and symptom appearance by summer drought stress resembles an annual time step, and data available for model fitting lacked seasonal resolution. An explicit representation of vector populations was not included because we had no information on key vector parameters such as densities, biting rates, or transmission efficiency. Instead, the role of vectors in transmitting the bacterial disease was implicitly captured in the frequency-dependent contact rate β of the epidemiological model, the form of which is often assumed for vector-borne diseases (Ferrari *et al*., 2011).

We model the numbers of susceptible and infected host plants in the olive groves. Model compartments were chosen to represent the major stages of disease progression in olive trees. A susceptible compartment (S_t) included the healthy uninfected trees at time t (years). To reflect the potential for differential infectiveness of olive trees at different stages of infection, the infected (I_t) compartment from the standard framework (Allen, 1994) was subdivided into three sequential compartments representing the numbers of infected trees without symptoms ('symptomless', $I_{A,t}$), with symptoms ('symptomatic', $I_{S,t}$), and with the majority or all of the branches dead ('desiccated', $I_{D,t}$). We expected that, compared to trees with symptoms, there would be lower infectivity from trees without symptoms because they have a low bacterial load (Saponari *et al*., 2017) and are probably less likely to transmit *X. fastidiosa* subsp. *pauca* to vector insects. Similarly, we expected desiccated trees to have lower infectivity because, although the bacterial load is likely to be high, much of the foliage is withered and brown, which probably makes the trees less attractive to vector insects and may support lower vector densities. Thus, we included in the model two proportion parameters, b_A and b_D, representing the relative infectiveness of infected symptomless and desiccated trees, respectively, as a proportion of the infectiveness of symptomatic trees.

A further modification to the standard compartmental model was made to characterize observed disease progression. In standard compartmental models (Allen, 1994), individuals may pass to the subsequent compartment immediately after entering their current compartment. In this case, transition times are exponentially distributed for continuous time models and geometrically distributed for discrete time models. However, the disease progression data indicated a delay between appearance of initial symptoms and onset of extensive symptom expression and rapid die back. This probably represents a minimum time period for bacterial load in the trees to build up to lethal levels. Therefore, we extended the basic compartmental model so that infected olive trees would not start to enter the desiccated I_D compartment until after a sojourned symptom expression period of τ years had passed (subsequently referred to as desiccation delay parameter). We denote the τ^{th} compartment of symptomatic sojournment by $I^{\tau}_{S,t}$. The total number of trees with symptoms is given by

$$I_{S,t} = \sum_{j=1}^{\tau+1} I^{j}_{S,t}$$

The epidemiological dynamics at population level are given by

$$S_{t+1} = (1-\alpha_t)\, S_t$$

$$I_{A,t+1} = (1-\sigma)\, I_{A,t} + \alpha_t S_t$$

$$I^{1}_{S,t+1} = \sigma I_{A,t}$$

$$I^{2}_{S,t+1} = I^{1}_{S,t}$$

$$\vdots$$

$$I^{\tau}_{S,t+1} = I^{\tau-1}_{S,t}$$

$$I^{\tau+1}_{S,t+1} = (1-\gamma)\, I^{\tau+1}_{S,t} + I^{\tau}_{S,t}$$

$$I_{D,t+1} = I_{D,t} + \gamma I^{\tau+1}_{S,t}$$

capturing the following individual annual transition probabilities for infection of susceptible trees (α_t), symptom appearance in symptomless infected trees (σ), and mortality of infected trees with symptoms (γ), which are given by

$$\alpha_t = 1 - e^{-\beta \frac{I_{S,t} + b_A I_{A,t} + b_D I_{D,t}}{N}}$$

$$\sigma = 1 - e^{-1/T_A}$$

$$\gamma = 1 - e^{-1/T_D}.$$

Here, $N_t = S_t + I_{A,t} + I_{S,t} + I_{D,t} = N$ is the total number of olive trees in the population. The contact rate β is the expected number of *Xylella*-transmitting contacts per year from each infective tree with symptoms (Allen, 1994) and, as explained above, proportions b_A and b_D scale the relative infectiveness of $I_{A,t}$ and $I_{D,t}$. Parameter T_A is

the mean duration of the symptomless period in years and T_D is the mean time to desiccation after τ years.

It can be seen from this that our model is a generalization of standard compartmental models in the Susceptible-Exposed-Infected-Removed (SEIR) framework (Allen, 1994) whereby the exposed and removed classes are able to infect the susceptible class. In the case that there is no delay ($\tau = 0$), the model collapses to a standard discrete-time compartmental model (Data S1). Setting $b_A = 0$ means that I_A is equivalent to an uninfectious exposed E compartment, while setting $b_D = 0$ means that I_D is equivalent to an uninfectious R compartment. When $b_A = 1$ or $b_D = 1$, I_A and I_D are, respectively, equally infectious as I_S and thus these compartments can be thought of as a single infected I compartment. It can be seen from this that fixing b_A and b_D individually to values of 0 or 1 we can convert our general model into forms resembling SI-like, SIR-like, SEI-like, and SEIR models. It should be noted that the SI-like, SIR-like, and SEI-like model simplifications retain additional model compartments compared to their classical counterparts (see Data S1). This allowed us to compare the fit of the full generalized model (hereafter referred to as the $SI_AI_SI_D$ model) to simpler variants, in order to assess the weight of evidence for the more complex model provided by available data, whilst retaining key infection dynamics and parsimony with the data structure.

2.2 | Data to estimate the model parameters

Models were fitted to data from 2 to 3 yearly censuses of symptom prevalence in 17 olive groves infected with *X. fastidiosa* subsp. *pauca* in Puglia, Italy. All trees were naturally infected and are situated within the demarcated infected zone in Puglia. The majority of the data came from 3 years of monitoring symptom progression in 3,335 olive trees in 16 infected olive groves containing susceptible olive cultivars (mean plot area 1.86 ± 1.57 ha, mean tree density 97.9 ± 41.7 trees/ha, typical of ancient olive groves in Puglia (EFSA Panel on Plant Health, 2019a). A subset of these data has previously been used to detect infection using airborne imaging spectroscopy and thermography (Zarco-Tejada *et al*., 2018), and earth observation satellite imagery (Hornero *et al*., 2020). The data consist of visual rating of disease severity for each tree, scored on a 0–5 canopy desiccation scale (see Zarco-Tejada *et al*., 2018, and Hornero *et al*., 2020, for a full description of the data). Maximum severity scores for each tree surveyed in late 2016 (June or October), 2017 (June, July, or December), and 2018 (July) were classified into compartments of the epidemiology model. Specifically, we chose severity score = 0 to represent both the uninfected susceptible (S) compartment and the infected symptomless compartment (I_A), severity score = 1–3 was regarded as being in the symptomatic infected (I_S) compartment and severity score = 4 (canopies with a prevalence of dead branches) or 5 (canopy completely dead) was regarded as the desiccated (I_D) compartment.

In addition, we used a census of disease symptoms from a single olive grove containing 187 trees from January 2014 and April 2015 at the early stages of infection. No desiccated trees were present, so all trees with symptoms were considered as being in the symptomatic infected (I_S) compartment.

2.3 | Model fitting and model comparison

The generalized $SI_AI_SI_D$model and its simplifications from the SEIR family (SI-like, SIR-like, SEI-like, and SEIR), all with a fixed range of values of the desiccation delay parameter, τ, were fitted to these data in a Bayesian framework. Then the fits of the candidate models were compared using the deviance information criterion (DIC) (Gelman *et al*., 2013) in order to identify the most parsimonious model structure and value of τ consistent with the data.

For any set of model parameters, we calculated deterministic disease dynamics for 12 years starting from an initial proportion of infected trees without symptoms, $I_{A,0}$, which was treated as an additional parameter to be estimated because it was not known when the trees became infected. Twelve years was considered an upper limit on the plausible length of time the plots could have been infected (Loconsole *et al*., 2014). The log-likelihood of the observed time series of symptomless trees, trees with symptoms, and desiccated trees from each plot were then estimated by aligning each plot's time series to the disease progression curves as well as possible. The optimal alignment was identified by calculating the log-likelihood of the observed numbers of trees without symptoms, with symptoms, and desiccated if their probabilities followed the model proportions of $S + I_A$, $S + I_A\ I_S$, and I_D compartments, respectively. The summed likelihood across plots was then calculated for optimization of the parameters. In effect, this approach estimates the time of infection of each plot as a latent variable.

Parameter estimation from these likelihoods was achieved using an adaptive Metropolis–Hastings MCMC sampler in which the variance–covariance matrix of the multivariate normal proposal distribution was tuned to an acceptance rate of 30% (Scheidegger, 2018). Each model was fitted with a chain of 10^6 iterations after a burn-in of 10^4 iterations and starting at maximum-likelihood parameters found by the Nelder–Mead simplex algorithm initiated from 100 random start parameterizations.

Parameters were estimated on their natural scales with uniform prior distributions (U) either spanning the full range of possible values (i.e., $U[0, 1]$ for the proportion parameters b_A, b_D, and $I_{A,0}$) or bounded at a lower value of 0 for strictly positive parameters. For β a prior distribution of $U(0, 1{,}000)$ was used, far exceeding the likely upper range for transmission rates. For T_D, a prior distribution of $U(0, 12)$ was used reflecting the duration of simulations. The exception to these extremely uninformative prior distributions was for T_A, for which a recent meta-analysis of literature data estimated a mean symptomless period for olive trees of 1.24 years (EFSA Panel on Plant Health, 2019a). Based on this information, we set the prior distribution for T_A to $U(0.75, 1.5)$ to allow for some degree of variance.

The adaptive MCMC sampler uses a multivariate normal proposal distribution for the parameters, which is not well suited to discrete parameter distributions. Therefore, we ran separate chains for

values of the desiccation delay parameter, τ, fixed at integer values between 0 and 6 years. For each model specification ($SI_AI_SI_D$, SI-like, SIR-like, SEI-like, and SEIR) the optimal value of τ was identified as that giving the minimal DIC, calculated using the variance of deviances in the MCMC chain (Gelman *et al*., 2013). Following this, the model specifications were then compared based on their DIC values.

2.4 | Sensitivity analysis

To assess the relative contribution of the model parameters to *X. fastidiosa* epidemics, we performed a sensitivity analysis on each fitted parameter, β, b_A, b_D, T_A, T_D, and $I_{A,0}$. Specifically, we compared relative changes (C) to the total change in susceptible and infected proportions over 12 simulated years (discrete area under the curve) relative to the median posterior valued scenario (p_0) for four different percentage changes in a single parameter value (p_v), where all other parameters remain at their median posterior value, such that

$$C_X = \frac{\sum_{t=0}^{t=12} X_t|_{p_v}}{\sum_{t=0}^{t=12} X_t|_{p_0}}, \text{ for } X \in \{S, I_A, I_S, I_D\},$$

where $X_t|_p$ are the output values (proportions in each model compartment) from simulating the epidemic model for a given set of parameter values, $p \in \{I_{A,0}, T_A, T_D, \beta, b_A, b_D\}$.

3 | RESULTS

3.1 | Model comparison

For all five epidemiological model specifications, MCMC chains had the lowest DIC when the desiccation delay parameter τ (the number of years with symptoms before desiccation begins) was set to 3 years (Table S1). In all cases, setting τ to a different value resulted in large increases in DIC of at least 7 units (Table S1) indicating very low support compared to models with $\tau = 3$ years.

With $\tau = 3$ years, comparison of the different epidemiological model specifications showed that the SEIR and SEI-like models gave the best fits to the data and were essentially indistinguishable from each other (Table 1). The full $SI_AI_SI_D$ model was slightly less parsimonious and was penalized for estimating two extra parameters that did little to differentiate the generalized model from the simpler SEI-like and SEIR models (Table S1). For example, the $SI_AI_SI_D$ model posterior median estimate of b_D (relative infectivity of desiccated trees) recapitulated its uniform prior distribution (Table 2, Figure 1), showing that this parameter has no effect on model fit and supporting the inability to distinguish between SEI-like and SEIR fits (Table 1). Furthermore, the $SI_AI_SI_D$ model posterior median estimate of b_A (relative infectivity of trees without symptoms) was very close to zero (Table 2) causing the trees without symptoms in the $SI_AI_SI_D$ model to function equivalently to the exposed (E) compartment of SEI-like and SEIR models. Supporting this, models in which trees without symptoms were fully infective (SI-like and SIR-like, with $b_A = 1$) gave the poorest fits to the data on the basis of DIC (Table 2).

3.2 | Parameter estimates and model dynamics

Posterior parameter estimates from the SEI-like and SEIR model were extremely similar (Table 2) and gave a very good fit to the observed disease progression in the monitored plots (Figures 2 and 3; Figure S1). The posterior for β suggested that an olive tree with symptoms is able to infect an average of 19.5 other trees in the local population each year (95% credible range 14–26; Table 2, Figure 1). The posterior distribution for T_A suggested a mean period without symptoms of around 1.2 years (14 months, 95% credible range 1.0–1.3 years; Table 2, Figure 1). Accounting for the 3-year delay before desiccation, the estimated mean time from symptom establishment to desiccation (τ+T_D) was 4.3 years (95% credible range 4.0–4.6 years;

TABLE 1 Comparison between the generalized full epidemiological model ($SI_AI_SI_D$) of *Xylella fastidiosa* infecting olive trees and simpler specifications, in which relative infectivity of symptomless or desiccated trees (b_A and b_D) are fixed rather than estimated

Model type[a]	Optimal delay (τ years)	DIC	ΔDIC	R^2		
				Symptomless trees	Trees with symptoms	Desiccated trees
SEI-like ($b_A = 0$, $b_D = 1$)	3	884.3	0.000	0.844	0.742	0.826
SEIR ($b_A = 0$, $b_D = 0$)	3	884.3	0.020	0.844	0.742	0.826
$SI_AI_SI_D$	3	889.8	5.504	0.838	0.730	0.825
SIR-like ($b_A = 1$, $b_D = 0$)	3	891.2	6.891	0.842	0.741	0.820
SI-like ($b_A = 1$, $b_D = 1$)	3	891.6	7.370	0.835	0.714	0.825

Note: For each model specification, MCMC chains were run with fixed values of the desiccation delay parameter (τ) between 0 and 6 years and the optimal value selected based on deviance information criteria (DIC). With these optimized values of τ, the alternative models are here ranked based on their DIC. Pseudo-R^2 values are the squared correlations between observed and fitted proportions of symptomless trees, trees with symptoms, and desiccated trees.

[a]SEIR, Susceptible-Exposed-Infected-Removed model; $SI_AI_SI_D$, Susceptible-Infected (symptomless)-Infected (symptomatic)-Infected (desiccated) model; b_A, infectivity of symptomless infected olive trees, relative to trees with symptoms; b_D, infectivity of desiccated olive trees, relative to trees with symptoms.

TABLE 2 Estimated epidemiological parameters from Bayesian model fitting to disease progression of *Xylella fastidiosa* in 17 olive grove plots

Parameter	Meaning	Posterior median [±95% interval]		
		$SI_AI_SI_D$ model	SEI-like model	SEIR model
β	Effective contact rate for infected olive trees with symptoms (per year)	17.88 [6.33–24.88]	19.49 [14.39–25.87]	19.45 [14.39–25.81]
b_A	Infectivity of symptomless infected olive trees, relative to trees with symptoms	0.015 [0.000–0.439]	–	–
b_D	Infectivity of desiccated olive trees, relative to trees with symptoms	0.503 [0.026–0.976]	–	–
T_A	Mean duration of the symptomless period (years)	1.187 [1.089–1.276]	1.180 [1.067–1.274]	1.179 [1.066–1.273]
T_D	Mean time to desiccation after τ years with symptoms (years)	1.360 [1.114–1.595]	1.339 [1.038–1.578]	0.006 [0.004–0.009]
$I_{A,0}$	Initial infection proportion	0.005 [0.003–0.008]	1.338 [1.039–1.579]	0.006 [0.004–0.009]

Note: The posterior medians and 95% intervals calculated from the posterior samples are given for the full generalized Susceptible-Infected (symptomless)-Infected (symptomatic)-Infected (desiccated) model ($SI_AI_SI_D$) and the simpler Susceptible-Exposed-Infected-Removed (SEIR) and SEI-like models in which b_A and b_D were fixed.

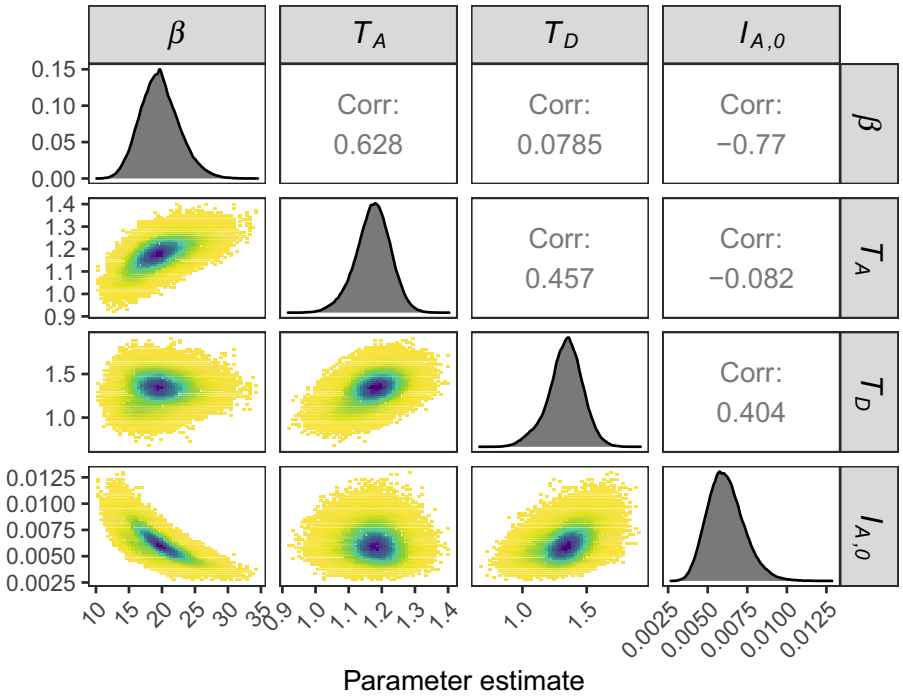

FIGURE 1 Parameter estimates, distributions and correlations for the Susceptible-Exposed-Infected (SEI)-like version of the epidemiological model for *Xylella fastidiosa* infecting olive trees. On the diagonal, pair plots show the posterior distributions of parameters from the SEI-like version of the model from 10^6 MCMC iterations. Below the diagonal, panels show the posterior correlations between parameter estimates (darker shading indicates greater posterior density), and panels above the diagonal give Pearson's correlation coefficients. β, effective contact rate for infected olive trees with symptoms (per year); T_A, mean duration of the symptomless period; T_D, mean time to desiccation after τ years with symptoms; I_A, proportion of infected trees without symptoms [Colour figure can be viewed at wileyonlinelibrary.com]

Table 2, Figure 1). Posterior estimates for the initially infected proportion ($I_{A,0}$) were very low (Table 2, Figure 1) and equate to approximately one tree being initially infected in the median-sized plot. There was appreciable posterior correlation between estimates for some parameters, most notably the strong negative correlation between β and $I_{A,0}$ and positive correlation between β and T_A (Figure 1) as these parameters modulate the speed of disease spread in the early stages of infection.

Model projections by the fitted SEI-like version of the full $SI_AI_SI_D$ model shows that the model closely matches the data from the aggregated data across all plots (Figure 4) and that variation in the joint posterior distributions did not much affect the expected disease progression.

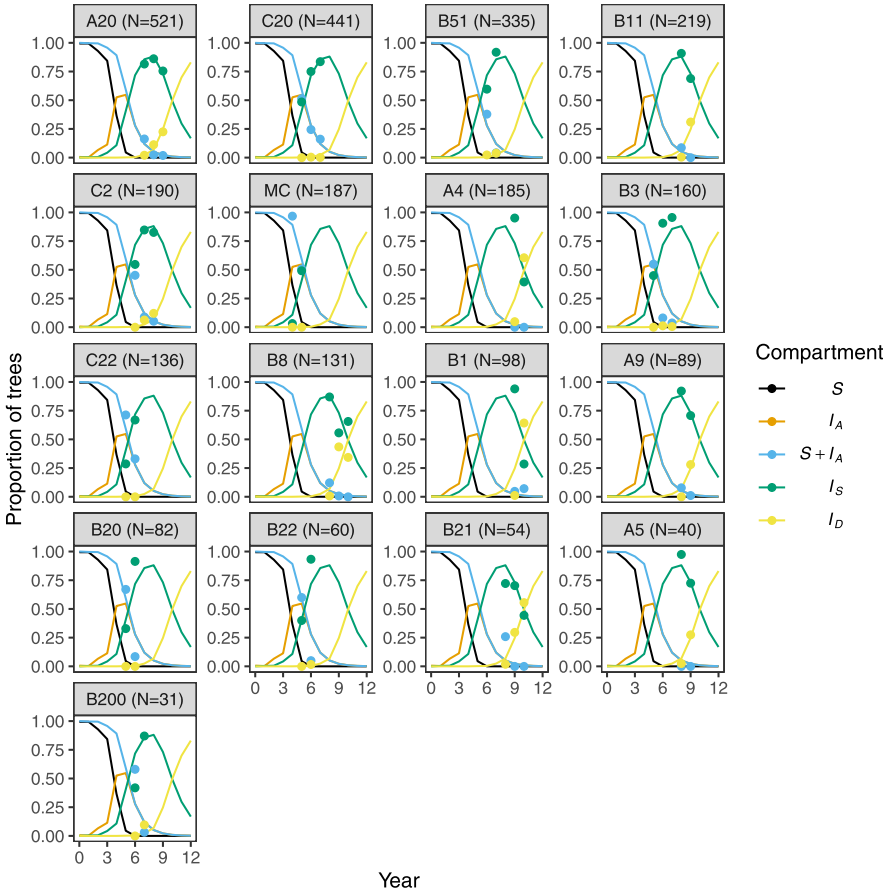

FIGURE 2 Observed and model-fitted disease progression of *Xylella fastidiosa* in 17 olive grove plots. The solid lines are the modelled disease dynamics with median posterior parameters of the best-fitting Susceptible-Exposed-Infected (SEI)-like version of the model and the points are the observed data from each plot aligned to the disease progression curve (labelled for each panel, along with number of trees, *N*). The observed data contained the proportion of all symptomless trees, corresponding to model compartments $S+I_A$, so this is also displayed. Model compartments shown are *S*, proportion of susceptible, uninfected trees; I_A, proportion of infected trees without symptoms; I_S, proportion of infected trees with symptoms; I_D, proportion of infected trees with the majority or all branches dead [Colour figure can be viewed at wileyonlinelibrary.com]

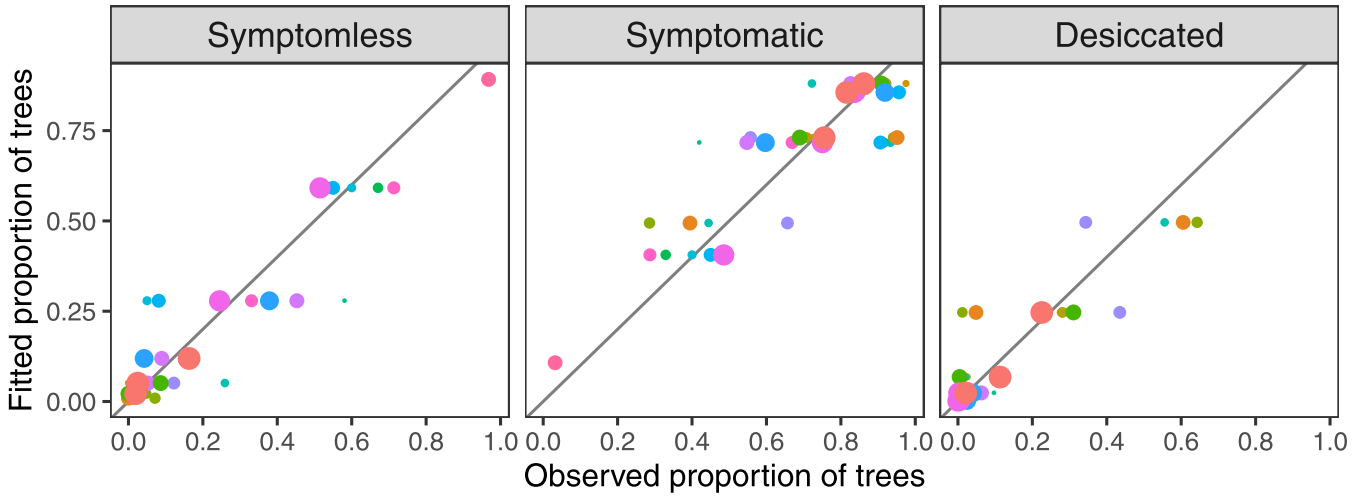

FIGURE 3 Comparison of observed and fitted proportions of olive trees infected with *Xylella fastidiosa* that were without symptoms, with symptoms, and desiccated (majority or all branches dead), from the Susceptible-Exposed-Infected (SEI)-like version of the model. Point sizes reflect numbers of trees surveyed and colours differentiate individual plots. The grey 1:1 line shows the correspondence between observed and fitted [Colour figure can be viewed at wileyonlinelibrary.com]

3.3 | Sensitivity analysis

The results of the sensitivity analysis for the full $SI_AI_II_D$ model is given in Figure 5 where we compare −50%, −10%, +10%, and +50% changes in individual median posterior parameter values given in Table 2 (comparable results for the SEI-like and SEIR models are presented in Figure S2). Results show that β and $I_{A,0}$ are the most sensitive parameters, where parameter increases result in decreases in total susceptible host plants and increases in infected host plants. Conversely, b_D is the least sensitive, showing little change in the model output. This is perhaps unsurprising given that b_D was found to be uninformative in the Bayesian model fitting (Table 2). Interestingly, other model parameters show sensitivity in particular infection compartments, but not in the overall infection as seen in

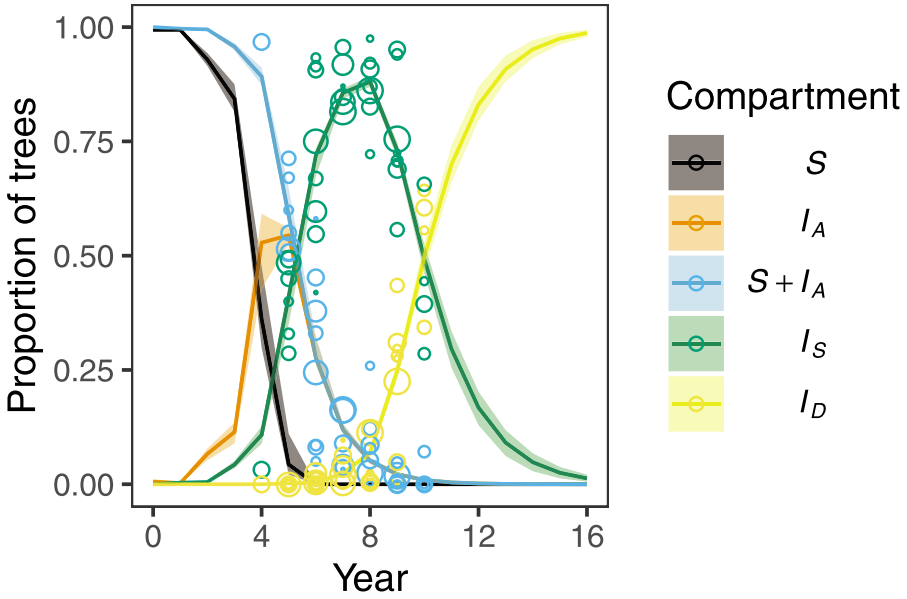

FIGURE 4 Model-fitted disease progression of *Xylella fastidiosa* infecting olive trees, from the Susceptible-Exposed-Infected (SEI)-like version of the model. Lines show the median predicted frequencies of each model compartment from 10,000 posterior samples, with ribbons showing the 95% credible intervals. Points are the observed proportions of trees without symptoms ($S+I_A$), with symptoms (I_S), and desiccated trees (I_D) from 17 plots, maximally aligned to the model progression curves during model fitting. Point sizes indicate the number of trees in each plot. *S*, susceptible uninfected trees; *I*, infected trees [Colour figure can be viewed at wileyonlinelibrary.com]

the changes in the susceptible compartment (recall, $I_A + I_S + I_D = N - S$). For example, changes in T_A cause large effects on the symptomless compartment (I_A), but less on the overall disease dynamics (*S*).

4 | DISCUSSION

X. fastidiosa is a devastating plant pathogen that has the potential to infect large numbers and species of cultivated and wild plants (European Food Safety Authority, 2018; EFSA Panel on Plant Health, 2019a). Due to the unpredictable nature of the Puglian outbreak (e.g., a new host, a novel location, conducive climate, etc.), mitigation strategies have mostly been underpinned by laboratory studies, or on studies from its previous range (European Food Safety Authority, 2018; EFSA Panel on Plant Health, 2019a, 2019b). Importantly, detailed quantified knowledge of the epidemiological progression in olive hosts in a field setting has been lacking, an omission that we have attempted to address here. In this paper we fitted mathematical epidemiological models to field data that detailed the level of symptoms expressed by the bacterial disease. In general, there is an inherent difficulty of model fitting for long-lived or emerging infectious diseases, where, typically, long time series are required to track full infection and mortality of a population (Meentemeyer *et al*., 2011). Here, we address that difficulty by analysing and fitting the models to short disease time series from multiple populations that capture the full range of disease dynamics (assuming similar underlying processes), thus effectively swapping space for time. When we compared the full model against simplified model versions to test how well the model was supported by the data, our selected model fitted the data well and estimated important epidemiological parameters.

One of the most critical epidemiological parameters to measure is the transmission rate, the rate at which susceptible hosts become infected, as this is a measure of disease spread, and strongly influences how difficult achieving control may be (Allen, 1994). We estimated that one infected symptomatic olive infected approximately 19 susceptible hosts per year, suggesting a fast rate of transmission. During the symptomless period, the bacterium begins to replicate within the host, colonizing large parts of the plant xylem (Saponari *et al*., 2017). Over this period the host plant is potentially infectious as it is possible for xylem-feeding insect vectors to take up the bacterium (Sicard *et al*., 2018). However, infectivity or transmission has not yet been directly estimated in laboratory or field experiments; thus, our model estimates are useful first attempts at quantifying this. We estimated from the $SI_AI_II_D$ model that the relative infection rate of olive trees without symptoms is, on average, approximately 1.5% of that of plants with symptoms; however, there is some degree of uncertainty in our estimates. Model selection and sensitivity analysis showed that the effects of symptomless infectivity are almost negligible, and therefore, we conclude it has little effect on overall epidemiological dynamics once the outbreak has established. Unfortunately, we were unable to ascertain the relative contribution of desiccated plants because there was insufficient information in the data to inform the parameter range. This was because delayed desiccation and rapid transmission led to all olives becoming infected before desiccation. However, it is likely that highly infected desiccated plants are less infectious than plants with symptoms,

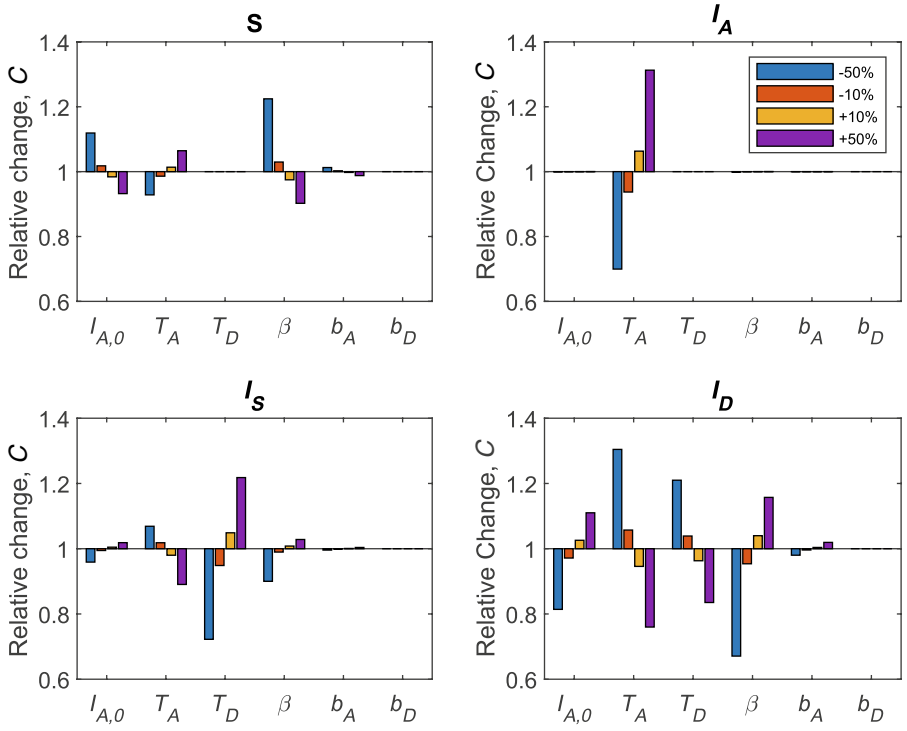

FIGURE 5 Sensitivity analysis of the Susceptible-Infected (symptomless)-Infected (symptomatic)-Infected (desiccated) (SI_AI_ID) epidemiological model for *Xylella fastidiosa* infecting olive trees. The analysis shows the relative changes (*C*) in total proportions of susceptible and infected host plants for percentage changes in parameter values for the SI_AI_ID model. $I_{A,0}$, Initial proportion of infected trees without symptoms; T_A, mean duration of the symptomless period; T_D, mean time to desiccation after τ years with symptoms; β, effective contact rate for infected olive trees with symptoms (per year); b_A, infectivity of symptomless infected olive trees, relative to trees with symptoms; b_D, infectivity of desiccated olive trees, relative to trees with symptoms [Colour figure can be viewed at wileyonlinelibrary.com]

because they are less attractive to vectors (Sicard *et al*., 2018); nevertheless, new shoots (i.e., suckers) that are infected, and develop symptoms later, could act as a reservoir for further transmission. Our sensitivity analysis revealed that the parameter has little effect on the model disease dynamics over a 12-year period, suggesting that desiccated plants may not play an important role in growth of local infection during the initial stages of an outbreak. Furthermore, given the substantial time to desiccation and that the speed of spread is often determined by the dynamics at the invasion wavefront (Kot and Schaffer, 1986), desiccated plants may also have little impact on long distance spread. However, failing to remove desiccated infectious trees could spawn new infections in uninfected trees, such as newly planted trees, as they could act as a disease reservoir.

Detecting the presence of infected plants for surveillance or control can require considerable costly resources. The problem is further compounded when the pest is not easily detectable, such as when symptoms are not visible (Mastin *et al*., 2019), although new remote-sensing technologies are being developed (Zarco-Tejada *et al*., 2018; Hornero *et al*., 2020). This challenge is especially important for biosecurity of imports, because long symptomless periods may result in the movement of infected materials without the knowledge of the importer or importee. Furthermore, outbreaks of disease may go unnoticed for a considerable time (Soubeyrand *et al*., 2018), making eradication difficult. Therefore, estimates of the symptomless period are critical for pest risk assessment (Thompson *et al*., 2016). Laboratory studies of plants infected with *X. fastidiosa* have estimated the symptomless period in susceptible olive cultivars to be approximately 14 months (c.1.2 years; Saponari *et al*., 2017; EFSA Panel on Plant Health, 2019a), with symptoms appearing after a longer delay in cultivars deemed resistant to *X. fastidiosa* subsp. *pauca* ST 53 (the causative agent of olive quick decline syndrome; Saponari *et al*., 2017). Although these laboratory studies where carried out with saplings in idealized conditions as opposed to mature trees in the field, our field estimates are in approximate agreement with their results. This alignment in our estimate gives some independent validation, and is clearly important for legislation because it has been shown that *X. fastidiosa* has one of the longest symptomless periods amongst some of the most dangerous plant diseases (EFSA Panel on Plant Health, 2019a). It should be noted that we used an informed prior distribution in our Bayesian framework, but the posterior distribution was shown to have a smaller credible interval, suggesting a high degree of confidence in model fitting.

Our analyses estimated that the mean time from early symptom expression to desiccation was approximately 4.3 years (τ+T_D). Furthermore, the findings are consistent with an approximately 3-year delay before the onset of rapid desiccation in mature olive trees. This is in line with our casual observations and those of others (Martelli, 2016), with area-wide rapid and relatively synchronized

desiccation events. Saponari *et al*. (2017) found that full desiccation in laboratory studies using saplings occurred after approximately 2 years. However, it is likely that time to desiccation in mature trees in the field is highly dependent on environmental factors, which may induce stress (e.g., water stress), and other factors such as the number and timings of inoculations from multiple vector bites, size, age, and health of the host plant, season, location of inoculum and prevalence of vectors, to name a few. Despite these factors, our time to desiccation estimate had a relatively narrow 95% confidence interval. This may be due to the fact that the data were collected from adjacent locations over the same period.

In Puglia, *P. spumarius* is the main vector of *X. fastidiosa* subsp. *pauca* (Saponari *et al*., 2014b; Cornara *et al*., 2017). Vector abundance is difficult to predict as their distribution is patchy (Morente *et al*., 2018), and female oviposition is not correlated with olive proximity (Latini *et al*., 2019). However, it has been shown that *P. spumarius* occurrence and abundance does increase with olive grove land cover, although evidence of other biotic and abiotic factors affecting insect populations is less well supported (Santoiemma *et al*., 2019). Based on this, and a lack of data on the abundance of insect vectors, we chose not to explicitly model vector dynamics (but see EFSA Panel on Plant Health, 2019a, for a seasonal vector model). One further caveat with our approach is that our data only relates to the symptoms expressed rather than a quantitative measure of bacterial load. This is especially important because symptomless plants may be either uninfected or infected without symptoms. We have attempted to counteract this in our fitting method by combining the two classes in the model when comparing it to the data with a severity score of zero.

X. fastidiosa has been predicted to be able to establish over wide geographical areas, with the most suitable environment in the Mediterranean basin (EFSA Panel on Plant Health, 2019a), even under climate change (Bosso *et al*., 2016). Whilst the current outbreaks represent a small fraction of this suitable region, the potential for spread is high, given the global increase in trade (Chapman *et al*., 2017; see Saponari *et al*., 2019, for example). Policies, as described in Decision (EU) 2015/789 and Decision (EU) 2017/2352 on the containment and eradication strategies in the event of a detection of *X. fastidiosa* in the EU, rely on accurate information. Our findings on key epidemiological parameters, such as the transmission rate at different stages of the disease, symptomless period, and time to death, help to achieve informed policy. These will be important for predicting the spread and control of this disease using spatially explicit landscape-scale models (White *et al*., 2017; Soubeyrand *et al*., 2018; Abboud *et al*., 2019; EFSA Panel on Plant Health, 2019a). Furthermore, these epidemiological parameters are difficult and costly to measure experimentally, but models fitted to monitoring data can provide estimates and uncertainty distributions, giving valuable knowledge on *X. fastidiosa* disease dynamics and, potentially, other plant diseases.

ACKNOWLEDGEMENTS

All authors are funded by the European Union's Horizon 2020 research and innovation programme under Grant Agreement No. 727987 – XF-ACTORS 'Xylella fastidiosa Active Containment Through a multidisciplinary-Oriented Research Strategy'. Field monitoring data was supported by Grant Agreement No. 635646 – POnTE 'Pest Organisms threaten Europe'. Support was also funded by grant agreement no. 734353 – CURE-XF 'Capacity Building and Raising Awareness in Europe and in Third Countries to Cope with *Xylella fastidiosa*'. We also acknowledge collaborations with the EFSA Plant Health Panel, especially Giuseppe Stancanelli, Stephen Parnell and Andrea Maiorano. We also thank Maria Saponari and Pierfederico La Notte for numerous useful discussions. Finally, we also thank the editor and two anonymous referees for their valuable comments. All authors confirm no conflict of interests.

DATA AVAILABILITY STATEMENT

The data that support the findings of this study are available from https://github.com/Quantalab/Xf-NPlants-2018/tree/master/data or the corresponding author upon request.

ORCID

Steven M. White https://orcid.org/0000-0002-3192-9969
Juan A. Navas-Cortés https://orcid.org/0000-0001-6480-1104
James M. Bullock https://orcid.org/0000-0003-0529-4020
Donato Boscia https://orcid.org/0000-0002-4544-8680
Daniel S. Chapman https://orcid.org/0000-0003-1836-4112

REFERENCES

Abboud, C., Bonnefon, O., Parent, E. and Soubeyrand, S. (2019) Dating and localizing an invasion from post-introduction data and a coupled reaction–diffusion–absorption model. *Journal of Mathematical Biology*, 79, 765–789.

Allen, L.J.S. (1994) Some discrete-time SI, SIR, and SIS epidemic models. *Mathematical Biosciences*, 124, 83–105.

Almeida, R.P.P. (2016) Can Apulia's olive trees be saved? *Science*, 353, 346–348.

Bosso, L., Di Febbraro, M., Cristinzio, G., Zoina, A. and Russo, D. (2016) Shedding light on the effects of climate change on the potential distribution of *Xylella fastidiosa* in the Mediterranean basin. *Biological Invasions*, 18, 1759–1768.

Chapman, D., Purse, B.V., Roy, H.E. and Bullock, J.M. (2017) Global trade networks determine the distribution of invasive non-native species. *Global Ecology and Biogeography*, 26, 907–917.

Cornara, D., Saponari, M., Zeilinger, A.R., de Stradis, A., Boscia, D., Loconsole, G *et al*. (2017) Spittlebugs as vectors of *Xylella fastidiosa* in olive orchards in Italy. *Journal of Pest Science*, 90, 521–530.

Daugherty, M.P. and Almeida, R.P.P. (2019) Understanding how an invasive vector drives Pierce's disease epidemics: seasonality and vine-to-vine spread. *Phytopathology*, 109, 277–285.

EFSA Panel on Plant Health (2019a) Update of the scientific opinion on the risks to plant health posed by *Xylella fastidiosa* in the EU territory. *EFSA Journal*, 17, e05665.

EFSA Panel on Plant Health (2019b) Effectiveness of *in planta* control measures for *Xylella fastidiosa*. *EFSA Journal*, 17, e05666.

European Food Safety Authority (2018) Update of the *Xylella* spp. host plant database. *EFSA Journal*, 16, e05408.

European Food Safety Authority (2020) Update of the *Xylella* spp. host plant database – systematic literature search up to 30 June 2019. *EFSA Journal*, 18, e06114.

Ferrari, M.J., Perkins, S.E., Pomeroy, L.W. and Bjørnstad, O.N. (2011) Pathogens, social networks, and the paradox of transmission scaling. *Interdisciplinary Perspectives on Infectious Diseases*, 2011, 267049.

Gelman, A., Carlin, J.B., Stern, H.S., Dunson, D.B., Vehtari, A. and Rubin, D.B. (2013) *Bayesian Data Analysis*, 3rd edition. Boca Raton, FL: CRC Press.

Gross, A., Holdenrieder, O., Pautasso, M., Queloz, V. and Sieber, T.N. (2014) *Hymenoscyphus pseudoalbidus*, the causal agent of European ash dieback. *Molecular Plant Pathology*, 15, 5–21.

Grünwald, N.J., Leboldus, J.M. and Hamelin, R.C. (2019) Ecology and evolution of the sudden oak death pathogen *Phytophthora ramorum*. *Annual Review of Phytopathology*, 57, 301–321.

Hornero, A., Hernández-Clemente, R., North, P.R.J., Beck, P.S.A., Boscia, D., Navas-Cortes, JA *et al.* (2020) Monitoring the incidence of *Xylella fastidiosa* infection in olive orchards using ground-based evaluations, airborne imaging spectroscopy and Sentinel-2 time series through 3-D radiative transfer modelling. *Remote Sensing of Environment*, 236, 111480.

Olivicola, I. (2019) *Xylella*, lo studio: 4 milioni di alberi morti e improduttivi, 50mila ettari desertificati, perso il 10% dell'olio italiano. Available at: https://www.italiaolivicola.it/news/comunicati-stampa/xylella-lo-studio-4-milioni-di-alberi-morti-e-improduttivi-50mila-ettari-desertificati-perso-il-10-dellolio-italiano/. [Accessed 24 June 2020]

Jones, K.E., Patel, N.G., Levy, M.A., Storeygard, A., Balk, D., Gittleman, JL *et al.* (2008) Global trends in emerging infectious diseases. *Nature*, 451, 990–993.

Kot, M. and Schaffer, W.M. (1986) Discrete-time growth-dispersal models. *Mathematical Biosciences*, 80, 109–136.

Latini, A., Foxi, C., Borfecchia, F., Lentinin, A., De Cecco, L., Iantosca, D *et al.* (2019) Tacking the vector of *Xylella fastidiosa*: geo-statistical analysis of long-term field observations on host plants influencing the distribution of *Phylaenus spumarius* nymphs. *Environmental Science and Pollution Research*, 26, 6503–6516.

Loconsole, G., Potere, O., Boscia, D., Altamura, G., Djelouah, K., Elbeaino, T *et al.* (2014) Detection of *Xylella fastidiosa* in olive trees by molecular and serological methods. *Journal of Plant Pathology*, 96, 7–14.

Martelli, G.P. (2016) The current status of the quick decline syndrome of olive in southern Italy. *Phytoparasitica*, 44, 1–10.

Mastin, A.J., Bosch, F.V.D., Berg, F.V.D. and Parnell, S.R. (2019) Quantifying the hidden costs of imperfect detection for early detection surveillance. *Philosophical Transactions of the Royal Society B: Biological Sciences*, 374, 20180261.

Meentemeyer, R.K., Cunniffe, N.J., Cook, A.R., Filipe, J.A.N., Hunter, R.D., Rizzo, DM *et al.* (2011) Epidemiological modeling of invasion in heterogeneous landscapes: spread of sudden oak death in California (1990–2030). *Ecosphere*, 2, art17. https://doi.org/10.1890/ES10-00192.1

Morente, M., Cornara, D., Plaza, M., Durán, J.M., Capiscol, C., Trillo, R *et al.* (2018) Distribution and relative abundance of insect vectors of *Xylella fastidiosa* in olive groves of the Iberian Peninsula. *Insects*, 9, 175.

Morgan, O. (2019) How decision makers can use quantitative approaches to guide outbreak responses. *Philosophical Transactions of the Royal Society B: Biological Sciences*, 374, 20180365.

Purcell, A.H. and Hopkins, D.L. (1996) Fastidious xylem-limited bacterial plant pathogens. *Annual Review of Phytopathology*, 34, 131–151.

Santoiemma, G., Tamburini, G., Sanna, F., Mori, N. and Marini, L. (2019) Landscape composition predicts the distribution of *Philaenus spumarius*, vector of *Xylella fastidiosa*, in olive groves. *Journal of Pest Science*, 92, 1101–1109.

Saponari, M., Boscia, D., Nigro, F. and Martelli, G. (2013) Identification of DNA sequences related to *Xylella fastidiosa* in oleander, almond and olive trees exhibiting leaf scorch symptoms in Apulia (southern Italy). *Journal of Plant Pathology*, 95, 668.

Saponari, M., Boscia, D., Loconsole, G., Palmisano, F., Savino, V., Potere, O *et al.* (2014a) New hosts of *Xylella fastidiosa* strain CoDiRO in Apulia. *Journal of Plant Pathology*, 96, 611.

Saponari, M., Loconsole, G., Cornara, D., Yokomi, R.K., De Stradis, A., Boscia, D. *et al.* (2014b) Infectivity and transmission of *Xylella fastidiosa* by *Philaenus spumarius* (Hemiptera: Aphrophoridae) in Apulia, Italy. *Journal of Economic Entomology*, 107, 1316–1319.

Saponari, M., Boscia, D., Altamura, G., Loconsole, G., Zicca, S., D'Attoma, G *et al.* (2017) Isolation and pathogenicity of *Xylella fastidiosa* associated to the olive quick decline syndrome in southern Italy. *Scientific Reports*, 7, 17723.

Saponari, M., D'Attoma, G., Abou Kubaa, R., Loconsole, G., Altamura, G., Zicca, S *et al.* (2019) A new variant of *Xylella fastidiosa* subspecies multiplex detected in different host plants in the recently emerged outbreak in the region of Tuscany, Italy. *European Journal of Plant Pathology*, 154, 1195–1200.

Scheidegger, A. (2018) adaptMCMC: Implementation of a generic adaptive Monte Carlo Markov chain sampler. Available from: https://CRAN.R-project.org/package=adaptMCMC. [Accessed 24 June 2020].

Schneider, K., van der Werf, W., Cendoya, M., Mourits, M., Navas-Cortes, J.A., Vicent, A *et al.* (2020) Impact of *Xylella fastidiosa* subspecies *pauca* in European olives. *Proceedings of the National Academy of Sciences of the United States of America*, 117, 9250–9259.

Sicard, A., Zeilinger, A.R., Vanhove, M., Schartel, T.E., Beal, D.J., Daugherty, MP *et al.* (2018) *Xylella fastidiosa*: Insights into an emerging plant pathogen. *Annual Review of Phytopathology*, 56, 181–202.

Soubeyrand, S., De Jerphanion, P., Martin, O., Saussac, M., Manceau, C., Hendrikx, P *et al.* (2018) Inferring pathogen dynamics from temporal count data: the emergence of *Xylella fastidiosa* in France is probably not recent. *New Phytologist*, 219, 824–836.

Thompson, R.N., Gilligan, C.A. and Cunniffe, N.J. (2016) Detecting presymptomatic infection is necessary to forecast major epidemics in the earliest stages of infectious disease outbreaks. *PLoS Computational Biology*, 12, e1004836.

Tumber, K.P., Alston, J.M. and Fuller, K. (2014) Pierce's disease costs California $104 million per year. *California Agriculture*, 68, 20–29.

White, S.M., Bullock, J.M., Hooftman, D.A.P. and Chapman, D.S. (2017) Modelling the spread and control of *Xylella fastidiosa* in the early stages of invasion in Apulia, Italy. *Biological Invasions*, 19, 1825–1837.

Zarco-Tejada, P.J., Camino, C., Beck, P.S.A., Calderon, R., Hornero, A., Hernández-Clemente, R *et al.* (2018) Previsual symptoms of *Xylella fastidiosa* infection revealed in spectral plant-trait alterations. *Nature Plants*, 4, 432–439.

SUPPORTING INFORMATION

Additional supporting information may be found online in the Supporting Information section.

How to cite this article: White SM, Navas-Cortés JA, Bullock JM, Boscia D, Chapman DS. Estimating the epidemiology of emerging *Xylella fastidiosa* outbreaks in olives. *Plant Pathol*. 2020;69:1403–1413. https://doi.org/10.1111/ppa.13238